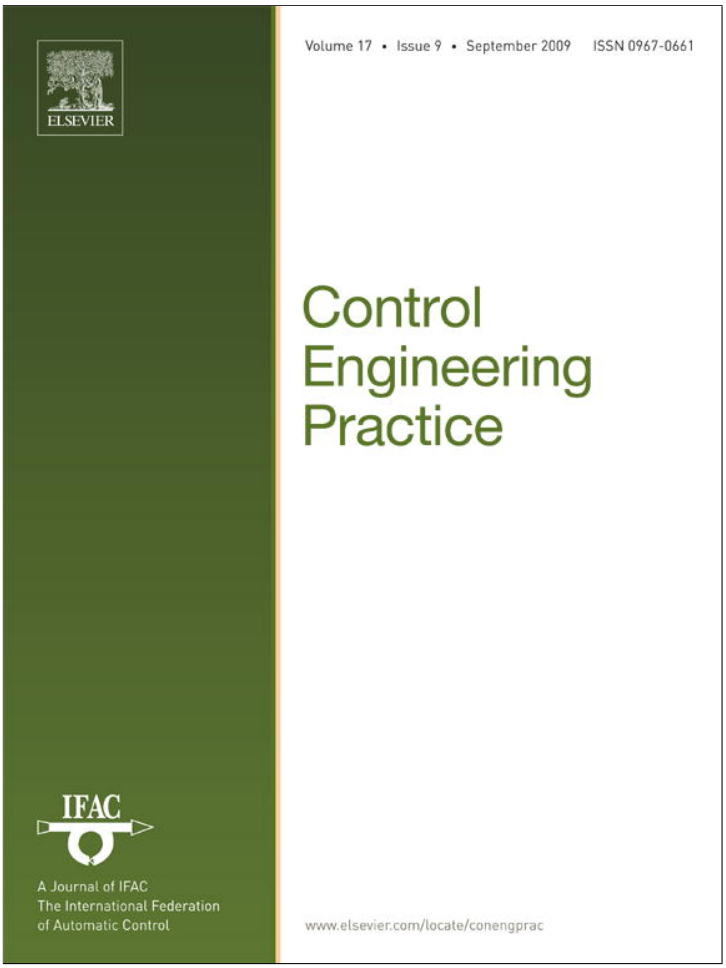

Control Engineering Practice 17 (2009) 1016–1025

Contents lists available at ScienceDirect

Control Engineering Practice

journal homepage: www.elsevier.com/locate/conengprac

# A practical approach to disturbance decoupling control

Qing Zheng [a], Zhongzhou Chen [b], Zhiqiang Gao [a,*]

[a] Center for Advanced Control Technologies, Department of Electrical and Computer Engineering, Cleveland State University, Cleveland, OH 44115, USA
[b] Department of Chemical Engineering, University of Massachusetts Amherst, Amherst, MA 01003, USA

ARTICLE INFO

*Article history:*
Received 2 April 2007
Accepted 16 March 2009
Available online 23 April 2009

*Keywords:*
Multivariable systems
Disturbance decoupling
Active disturbance rejection
Disturbance observer
Uncertain systems

ABSTRACT

In this paper, a unique dynamic disturbance decoupling control (DDC) strategy, based on the active disturbance rejection control (ADRC) framework, is proposed for square multivariable systems. With the proposed method, it is shown that a largely unknown square multivariable system is readily decoupled by actively estimating and rejecting the effects of both the internal plant dynamics and external disturbances. By requiring as little information on plant model as possible, the intention is to make the new method practical. The stability analysis shows that both the estimation error and the closed-loop tracking error are bounded and the error upper bounds monotonously decrease with the bandwidths. Simulation results obtained on two chemical process problems show good performance in the presence of significant unknown disturbances and unmodeled dynamics.



## 1. Introduction

Multi-input multi-output (MIMO) systems, also known as multivariable systems, permeate industry. The interactions or cross-couplings among various inputs and outputs of a system make design technologies in multivariable control systems fundamentally different from single-input single-output (SISO) control systems. Given that the understanding of the physics of MIMO systems usually helps the identification of the dominant input–output pairs, one design strategy is to disentangle the interactions among various input–output pairs and reduce a multivariable system into a number of independent SISO systems. This strategy is usually known as *decoupling*; but to avoid the confusion that could arise from the wide use of the term in process control pertaining to pre-compensation, the term *disturbance decoupling* is employed in this paper. Granted such a strategy is not the only one available, but it is a method of choice in some sectors in industry, such as those concerned with controls of chemical processes.

Decoupling of linear time invariant (LTI) multivariable systems has drawn researchers' interest in the past several decades (Descusse, 1991; Gilbert, 1969; Lu, 2008; Morgan, 1964; Morse & Wonham, 1970; Wang, 2003; Williams & Antsaklis, 1986; Zheng, Wang, & Lee, 2002), making it a well established area. The premise, however, is that the system is well represented by a LTI model. Robustness, disturbance rejection, and other practical concerns continue to pose serious challenges (Wang, 2003). For this reason, disturbance rejection is still a main concern in control system design (Astrom & Hagglund, 1995; Luyben, 1990; Takatsu & Itoh, 1999; Yang & Lo, 2008). In conjunction with decoupling control, the importance of disturbance rejection has been recognized by many researchers. One main disturbance rejection methods for decoupling control is based on the concept of the disturbance estimation. Several classes of approach are outlined below, including the unknown input observer (UIO) (Johnson, 1976), the disturbance observer (DOB) (Schrijver & van Dijk, 2002), the perturbation observer (POB) (Kwon & Chung, 2003), and the extended state observer (ESO) (Gao, 2003, 2006; Gao, Huang, & Han, 2001; Han, 1998, 1999). UIO is the disturbance estimator where the external disturbance is formulated as an augmented state and estimated using a state observer. DOB is another main class of disturbance estimators, based on the inverse of the nominal transfer function of the plant. POB is another class of disturbance estimators, similar to DOB in concept but formulated in state space in discrete time domain. Similar to UIO, ESO is also a state space approach. What sets ESO apart from UIO and DOB is that it is conceived to estimate not only the external disturbance but also plant dynamics. The effectiveness of UIO, DOB, and POB is limited by the requirement of an accurate mathematical model of the plant. In engineering practice, however, such presumption is hardly warranted as many industrial processes are highly uncertain and are in a perpetual flux.

In this paper, a novel disturbance rejection based approach is proposed where the cross-couplings between control loops as well as external disturbances are treated as "disturbance", estimated in real time and rejected. This *disturbance decoupling control* (DDC) strategy is rooted in a recently proposed novel control method: active disturbance rejection control (ADRC). Using ESO as the observer, the new method requires very little information of the plant dynamics. The original concept of active

* Corresponding author. Tel.: +1 216 687 3528; fax: +1 216 687 5405.
*E-mail address:* z.gao@csuohio.edu (Z. Gao).

0967-0661/$ - see front matter © 2009 Elsevier Ltd. All rights reserved.
doi:10.1016/j.conengprac.2009.03.005

disturbance rejection was proposed by Han (Gao et al., 2001; Han, 1998, 1999). Although the idea is quite imaginative, the nonlinear structure and a large number of tuning parameters, which need to be manually adjusted in implementation, make its large scale practical applications challenging. Recently, a new parameterization and tuning method was proposed, which greatly simplified the implementation of ADRC and made the design transparent to practicing engineers (Gao, 2003, 2006). More importantly, with the proposed parameterization of ADRC, it becomes a viable candidate for decoupling control.

ADRC is a quite different design philosophy. At its foundation is the recognition that, in the real world, dynamic systems are often highly uncertain, both in terms of the internal dynamics and external disturbances. The magnitude of the uncertainties could make them well beyond the reach of prevailing robust control theories, such as $H_2/H_\infty$. ADRC offers a solution where the necessary modeling information needed for the feedback control system to function well is obtained through the input–output data of the plant in real time. Consequently, the control system can react promptly to the changes either in the internal dynamics of the plant, or its external disturbances. It has been applied in many real systems (Su et al., 2004; Zheng & Gao, 2006). As first shown in Huang, Xu, Han, and Lam (2001) for aircraft flight control and then in Miklosovic and Gao (2005) for the jet engine problem, ADRC is a natural solution to disturbance decoupling control problems in the presence of large uncertainties. Compared to the above problems, the dynamics of some industrial systems, such as chemical processes, is even more nonlinear with less information available on how each input affects various outputs, which is needed to be known in the method used in Huang et al. (2001) and Miklosovic and Gao (2005). To address such challenges, a dynamic DDC approach is proposed in this paper. With little modeling information assumed, namely the predetermined input–output paring, the decoupling problem is reformulated as that of disturbance rejection, where disturbance is defined as the cross channel interference. The effect of one input to all other outputs that it is not paired with is viewed as a disturbance to be rejected. In the ADRC framework, such disturbance is actively estimated using ESO and canceled in the control law, in the absence of an accurate mathematical model of the plant.

The paper is organized as follows. It is shown how a disturbance decoupling problem can be reformulated and solved as a disturbance rejection problem in Section 2. Two case studies of chemical process control problems are performed for both linear and nonlinear multivariable systems, as shown in Section 3. Finally, some concluding remarks are given in Section 4. The stability characteristics of the proposed method is analyzed in Appendix A.

## 2. A dynamic disturbance decoupling control method

### 2.1. Reformulation of disturbance decoupling control problem

ADRC is a relatively new control design concept. In this paper, ADRC based DDC approach is proposed to address the decoupling problem for systems with large uncertainties of the internal dynamics and significant unknown external disturbances. Let

$$\begin{aligned}
&\vartheta_1 = [y_1^{(n_1-1)}(t), y_1^{(n_1-2)}(t), \ldots, y_1(t)],\\
&\vartheta_2 = [y_2^{(n_2-1)}(t), y_2^{(n_2-2)}(t), \ldots, y_2(t)],\\
&\quad\vdots\\
&\vartheta_m = [y_m^{(n_m-1)}(t), y_m^{(n_m-2)}(t), \ldots, y_m(t)],\\
&u = [u_1(t), u_2(t), \ldots, u_m(t)],\\
&w = [w_1(t), w_2(t), \ldots, w_m(t)].
\end{aligned} \tag{1}$$

Consider a system formed by a set of coupled input–output equations with predetermined input–output parings

$$\begin{cases}
y_1^{(n_1)} = f_1(\vartheta_1, \vartheta_2, \ldots, \vartheta_m, w, u) + b_{11}u_1\\
y_2^{(n_2)} = f_2(\vartheta_1, \vartheta_2, \ldots, \vartheta_m, w, u) + b_2u_2\\
\quad\vdots\\
y_m^{(n_m)} = f_m(\vartheta_1, \vartheta_2, \ldots, \vartheta_m, w, u) + b_{mm}u_i
\end{cases} \tag{2}$$

where $y_i$ is the output, $u_i$ the input, $w_i$ the external disturbances of the $i$th loop, respectively, $y_i^{(n_i)}$ denotes the $n_i$th order derivative of $y_i$, $i = 1, 2, \ldots, m$, and $f_i$ represents the combined effect of internal dynamics and external disturbances in the $i$th loop, including the cross channel interference. Note that $i$ refers to $i = 1, 2, \ldots, m$ in the following. In (2), it is assumed that the numbers of inputs and outputs are the same; the order $n_i$ and the input gain $b_{ii}$ are given.

A presumption in most existing decoupling control approaches is that an accurate mathematical model of the plant has been obtained. This could pose some rather considerable challenges time and cost wise in engineering practice. This is where the ADRC concept comes in. The idea is: if there is a viable alternative which can be used to realistically estimate $f_i$ in real time from input–output data, then the accurate mathematical description of $f_i$ might not be required. It is the aim of this paper to establish that ESO is indeed a suitable solution for this task.

### 2.2. Extended state observer

Instead of identifying the plant dynamics off-line, ESO is proposed to estimate the combined effect of plant dynamics and external disturbance in real time. The concept is introduced as follows.

The square multivariable system (2) is an $m$-loop system. An ADRC based SISO controller is designed for each loop independently. Consider the $i$th loop in (2)

$$y_i^{(n_i)} = f_i + b_{ii}u_i. \tag{3}$$

Let $x_{1,i} = y_i, x_{2,i} = \dot{y}_i, \ldots, x_{n_i,i} = y_i^{(n_i-1)}$ and $x_{n_i+1,i} = f_i$, which is added as an extended state. Assuming $f_i$ is differentiable, define

$$h_i = \frac{df_i}{dt} = \dot{f}_i. \tag{4}$$

Then (3) can also be represented in state space form as

$$\begin{aligned}
&\dot{x}_{1,i} = x_{2,i}\\
&\quad\vdots\\
&\dot{x}_{n_i-1,i} = x_{n_i,i}\\
&\dot{x}_{n_i,i} = x_{n_i+1,i} + b_{ii}u_i\\
&\dot{x}_{n_i+1,i} = h_i\\
&y_i = x_{1,i}
\end{aligned} \tag{5}$$

where $x_i = [x_{1,i}, x_{2,i}, \ldots, x_{n_i+1,i}]^T \in \mathbb{R}^{n_i+1}$, $u_i \in \mathbb{R}$, and $y \in \mathbb{R}$. An ESO for (5) is designed as

$$\begin{aligned}
&\dot{\hat{x}}_{1,i} = \hat{x}_{2,i} + l_{1,i}(x_{1,i} - \hat{x}_{1,i})\\
&\quad\vdots\\
&\dot{\hat{x}}_{n_i-1,i} = \hat{x}_{n_i,i} + l_{n_i-1,i}(x_{1,i} - \hat{x}_{1,i})\\
&\dot{\hat{x}}_{n_i,i} = \hat{x}_{n_i+1,i} + l_{n_i,i}(x_{1,i} - \hat{x}_{1,i}) + b_{ii}u_i\\
&\dot{\hat{x}}_{n_i+1,i} = l_{n_i+1,i}(x_{1,i} - \hat{x}_{1,i})
\end{aligned} \tag{6}$$

where $\hat{x}_i = [\hat{x}_{1,i}, \hat{x}_{2,i}, \ldots, \hat{x}_{n_i+1,i}]^T \in \mathbb{R}^{n_i+1}$ and $L_i = [l_{1,i}, l_{2,i}, \ldots, l_{n_i,i}, l_{n_i+1,i}]^T$ are the observer gain parameters to be chosen. In particular, let us consider a special case where the gains are

chosen as

$$[l_{1,i}, l_{2,i}, \ldots, l_{n_i,i}, l_{n_i+1,i}]^T = [\omega_{o,i}\alpha_{1,i}, \omega_{o,i}^2\alpha_{2,i}, \ldots, \omega_{o,i}^{n_i+1}\alpha_{n_i+1,i}]^T \quad (7)$$

with $\omega_{o,i}>0$. Here $\alpha_{j,i}$, $j=1,2,\ldots,n_i+1$ are chosen such that $s^{n_i+1}+\alpha_{1,i}s^{n_i}+\cdots+\alpha_{n_i,i}s+\alpha_{n_i+1,i}$ is Hurwitz. For simplicity, let $s^{n_i+1}+\alpha_{1,i}s^{n_i}+\cdots+\alpha_{n_i,i}s+\alpha_{n_i+1,i}=(s+1)^{n_i+1}$ where $\alpha_{j,i}=(n_i+1)!/(j!(n_i+1-j)!)$, $j=1,2,\ldots,n_i+1$. It results in the characteristic polynomial of (6) to be

$$\lambda_{o,i}(s)=s^{n_i+1}+\omega_{o,i}\alpha_{1,i}s^{n_i}+\cdots+\omega_{o,i}^{n_i+1}\alpha_{n_i+1,i}=(s+\omega_{o,i})^{n_i+1}. \quad (8)$$

This makes $\omega_{o,i}$, which is the observer bandwidth of the $i$th loop, the only tuning parameter for the $i$th loop observer and the implementation process much simplified, compared to other observers. Generally, the larger the observer bandwidth, the more accurate the estimation. However, a large observer bandwidth will increase noise sensitivity. Therefore a proper observer bandwidth should be selected in a compromise between tracking performance and the noise tolerance.

### 2.3. Dynamic disturbance decoupling

With a well-tuned observer, the observer states will closely track the states of the augmented plant. By canceling the effect of $f_i$ using $\hat{f}_i$, i.e, $\hat{x}_{n_i+1,i}$, ADRC actively compensates for $f_i$ in real time. The control law of the $i$th loop is designed as follows. The ADRC control law is given by

$$u_i=\frac{k_{1,i}(r_i-\hat{x}_{1,i})+\cdots+k_{n_i,i}(r_i^{(n_i-1)}-\hat{x}_{n_i,i})-\hat{x}_{n_i+1,i}+r_i^{(n_i)}}{b_{ii}} \quad (9)$$

where $r_i$ is the desired trajectory and $k_{j,i}$, $j=1,2,\ldots,n_i$ are the controller gain parameters. The closed-loop system becomes

$$y_i^{(n_i)}=(f_i-\hat{x}_{n_i+1,i})+k_{1,i}(r_i-\hat{x}_{1,i})+\cdots+k_{n_i,i}(r_i^{(n_i-1)}-\hat{x}_{n_i,i})+r_i^{(n_i)}. \quad (10)$$

Note that with a well-designed ESO, the first term in the right hand side (RHS) of (10) is negligible and the rest of the terms in the RHS of (10) constitute a PD controller with a feedforward term. Here $k_{j,i}$, $j=1,2,\ldots,n_i$ are the controller gain parameters selected to make $s^{n_i}+k_{n_i,i}s^{n_i-1}+\cdots+k_{1,i}$ Hurwitz. To further reduce the tuning parameters, all the controller poles are placed at $-\omega_{c,i}$. Then the approximate closed-loop characteristic polynomial becomes

$$\lambda_{c,i}(s)=s^{n_i}+k_{n_i,i}s^{n_i-1}+\cdots+k_{1,i}=(s+\omega_{c,i})^{n_i} \quad (11)$$

where $k_{j,i}=(n_i!/((j-1)!(n_i+1-j)!))\omega_{c,i}^{n_i+1-j}$, $j=1,2,\ldots,n_i$. This makes $\omega_{c,i}$, which is the controller bandwidth, the only tuning parameter for the $i$th loop controller. The controller bandwidth is selected based on how fast and steady that the output is needed to track the set point. A large controller bandwidth generally increases the response speed but, pushed to the limit, it also could make the system oscillatory, or even unstable. Thus the controller bandwidth is tuned based on the competing requirements of performance and stability margin, together with noise sensitivity as well. In addition, a large controller bandwidth usually increases the magnitude and rate of change in control signal and therefore the operation cost.

The primary reason for the above particular way of selecting $\alpha_{j,i}$ and $k_{j,i}$ is practicality: the observer and feedback gains must be easily tunable by the users. Another reason for such parameterization is that it reduces tuning to adjusting parameters that are familiar to engineers: bandwidth. It is advantageous that engineers could use a completely new design method without losing the critical insight gained from classical control: frequency response.

The convergence for the estimation error of the ESO and the closed-loop tracking error of DDC is shown in Appendix A.

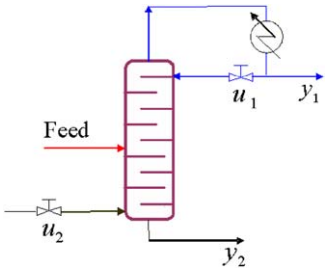


**Fig. 1.** A simplified scheme of distillation column.

## 3. Case studies

### 3.1. A linear multivariable system

A square multivariable system with two inputs and two outputs is illustrated how a linear MIMO system can be controlled by the proposed DDC framework. Distillation columns are very commonly used separation equipment in chemical and process industries. Fig. 1 shows a simplified scheme of distillation column. A stream of mixture enters the column in the middle and two products exit. The light product is drawn from the top and the heavy product is obtained from the bottom. The objective of the controller is to keep the purity of light product $y_1$ and the purity of heavy product $y_2$ at their desired values by manipulating the reflux flow rate $u_1$ and steam flow rate $u_2$. Generally, the feed flow rate is fixed. In case that the upstream process changes, the feed flow rate may have a disturbance.

In this paper, the Wood-Berry model of a pilot-scale distillation column (Wood & Berry, 1973) with delay set to zero is considered, which is shown as below:

$$\begin{bmatrix}y_1(s)\\y_2(s)\end{bmatrix}=\begin{bmatrix}\frac{K_{11}}{T_{11}s+1} & \frac{K_{12}}{T_{12}s+1}\\ \frac{K_{21}}{T_{21}s+1} & \frac{K_{22}}{T_{22}s+1}\end{bmatrix}\begin{bmatrix}u_1(s)\\u_2(s)\end{bmatrix} \quad (12)$$

where $K_{11}=12.8$, $K_{12}=-18.9$, $K_{21}=6.6$, $K_{22}=-19.4$, $T_{11}=16.7$, $T_{12}=21$, $T_{21}=10.9$, $T_{22}=14.4$. The system (12) can be represented as

$$\begin{cases}\dot{y}_1(t)=f_1+\frac{K_{11}}{T_{11}}u_1(t)\\ \dot{y}_2(t)=f_2+\frac{K_{22}}{T_{22}}u_2(t)\end{cases} \quad (13)$$

which is the form of (2). Note $f_1$ and $f_2$ account for all other factors except $u_1$ and $u_2$ in Loop 1 and Loop 2, respectively.

#### 3.1.1. Setpoint tracking and disturbance rejection performance

Let setpoints: $r_1=0$, $r_2=1$. Unmeasured trapezoidal disturbances are added into the system using look-up table definition in Simulink as follows:

$t=[0\ \ 50\ \ 60\ \ 90\ \ 100\ \ 200]$

$$d=\begin{bmatrix}0 & 0 & \begin{bmatrix}\frac{K_{d1}}{T_{d1}s+1}\\ \frac{K_{d2}}{T_{d2}s+1}\end{bmatrix}d_{mag} & \begin{bmatrix}\frac{K_{d1}}{T_{d1}s+1}\\ \frac{K_{d2}}{T_{d2}s+1}\end{bmatrix}d_{mag} & 0 & 0\end{bmatrix}$$

where $K_{d1}=3.8$, $K_{12}=4.9$; $T_{d1}=14.9$, $T_{d2}=13.2$; $d_{mag}=0.735$. The comparisons of disturbance rejection performance between the proposed DDC approach and MPC for Loop 1 and Loop 2 of

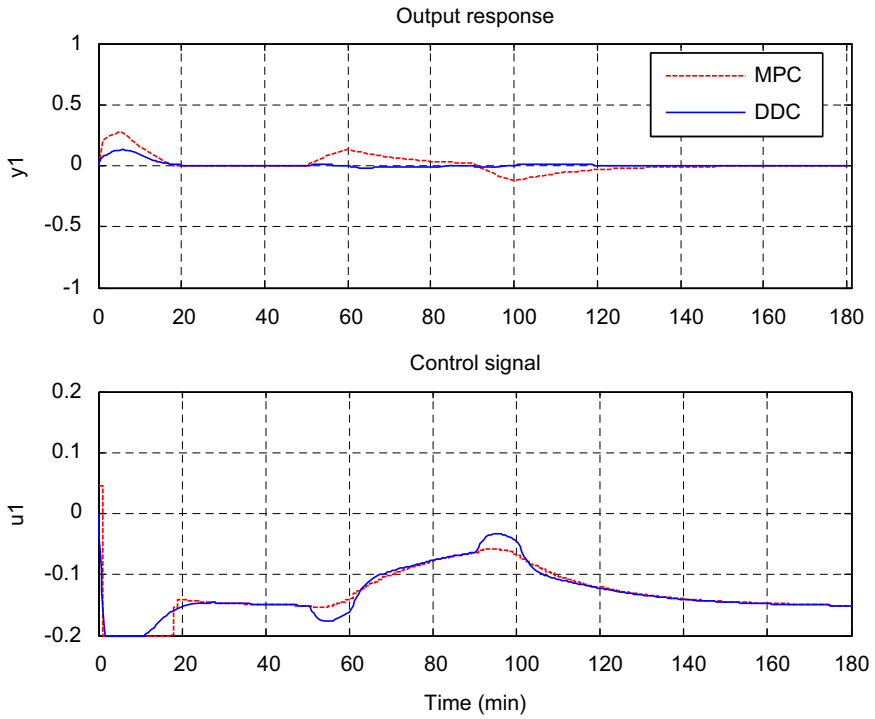


**Fig. 2.** The comparison of disturbance rejection performance between DDC and MPC for Loop 1 of the distillation column.

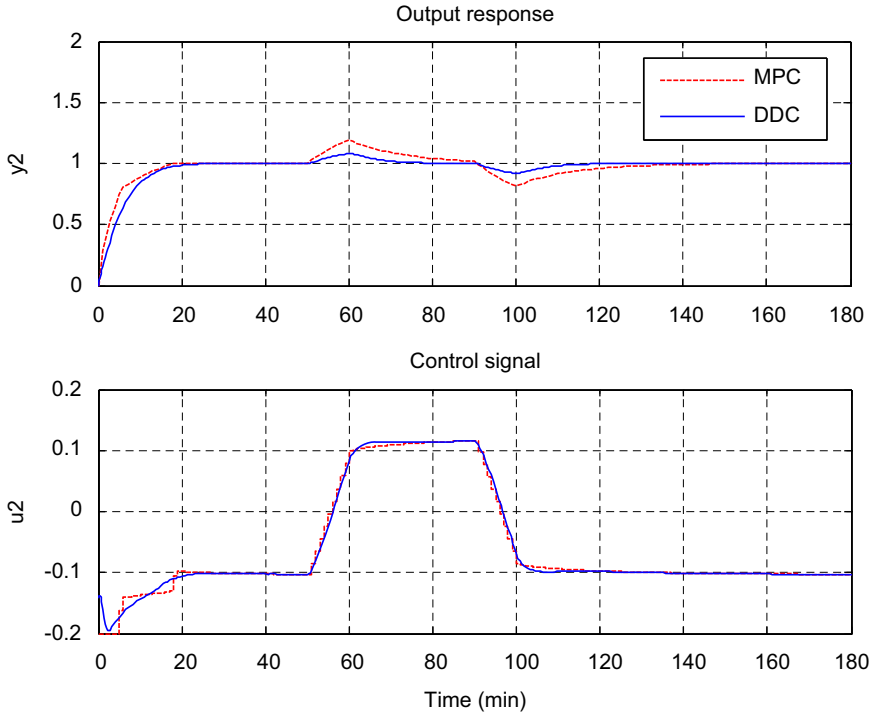


**Fig. 3.** The comparison of disturbance rejection performance between DDC and MPC for Loop 2 of the distillation column.

the distillation column are shown in Figs. 2 and 3, respectively. Their respective design or tuning parameters are as below. DDC parameters: $\omega_{c1} = \omega_{c2} = 0.2$, $\omega_{o1} = \omega_{o2} = 3$, $b_{0,11} = 0.8$, $b_{0,22} = -1.4$. Note that $b_{0,11}$ and $b_{0,22}$ are the approximate values of $b_{11}$ and $b_{22}$ in (13). MPC parameters: model horizon: 120, sampling rate: 1 min, prediction horizon: 90, control move horizon: 30, output weightings: [1 1], and control weightings: [0.1, 0.1]. Figs. 2 and 3 show that the DDC achieves better performance than MPC in disturbance rejection.

### 3.1.2. *Control signal selection*

In practice, it is sometimes difficult to decide which control signal should be chosen for one specific loop in the absence of the

plant model information. With the proposed DDC approach, the question becomes what happens when the pairing is chosen inappropriately. Consider the system

$$\begin{cases} \dot{y}_1 = f_{1nou} + b_{11}u_1 + b_{12}u_2 \\ \dot{y}_2 = f_{2nou} + b_{21}u_1 + b_{22}u_2 \end{cases} \tag{14}$$

where $b_{12} = 5b_{11}$, $b_{21} = 5b_{22}$, $u_1$ is the control signal of Loop 1, and $u_2$ is the control signal of Loop 2. That is, a clearly wrong choice was made regarding which input is the primary control signal for each loop. Here $f_{1nou}$ and $f_{2nou}$ represent the unknown system dynamics. The output performance and control signal with DDC are shown in Fig. 4. It can be observed that the control signals for both loops become more aggressive, or, in other words, more costly compared to the previous case, indicating that while using non-dominant control signals are not necessarily detrimental, they are certainly to be avoided as much as possible.

### 3.2. A nonlinear multivariable system

The continuous stirred tank reactor (CSTR) is widely used in chemical and process industries and it is a significant benchmark problem in process control. The system studied here is a CSTR with an irreversible exothermic first order reaction $A \rightarrow B$ (Dayal & MacGregor, 1997). Fig. 5 shows the CSTR diagram. A pure stream of species A enters a constant volume reactor and a well-mixed stream of species $A$ and $B$ exit the reactor. The control objective is to keep the reactor concentration $C_A$ and the reactor temperature $T$ at their desired settings. The manipulated variables are the reactant feed flow rate $F_{in}$ and the coolant water mass rate at the inlet $F_w$.

According to the reactant mass balance, reactor energy balance and the cooling jacket energy balance, a dynamic model of the plant is obtained. The plant model can be written into a standard nonlinear system representation as the following (Roffel & Betlem, 2004):

$$\dot{x} = \begin{bmatrix} -rx_1 \\ \dfrac{-V\Delta Hrx_1 + UA(x_3 - x_2)}{V\rho C_p} \\ \dfrac{UA(x_2 - x_3)}{V_j\rho_w C_{pw}} \end{bmatrix} + \begin{bmatrix} \dfrac{C_{A,in} - x_1}{V} & 0 \\ \dfrac{T_{in} - x_2}{V} & 0 \\ 0 & \dfrac{T_w - x_3}{V_j\rho_w} \end{bmatrix} u$$

$$[y_1 \;\; y_2]^T = \begin{bmatrix} \dfrac{C_{A,in} - x_1}{C_{A,in}} & x_2 \end{bmatrix}^T \tag{15}$$

where

$$r = k_0 \exp\left(\frac{-E}{Rx_2}\right),$$

$$x = [x_1, x_2, x_3]^T = [C_A, T, T_j]^T,$$

$$u = [u_1, u_2]^T = [F_{in}, F_w]^T.$$

The description of variables for this CSTR model is given in Roffel and Betlem (2004), which is also listed in Appendix B. The nonlinear is unmistakable by observing Eq. (15); note that the B matrix contains in it elements of the state vector and the coefficient $r$ is a nonlinear function of $x_2$.

The output responses of CSTR under the control of the DDC with two different sets of tuning parameters are shown in Fig. 6. The control signals of CSTR are shown in Fig. 7. The tracking error of CSTR is shown in Fig. 8. The design parameters

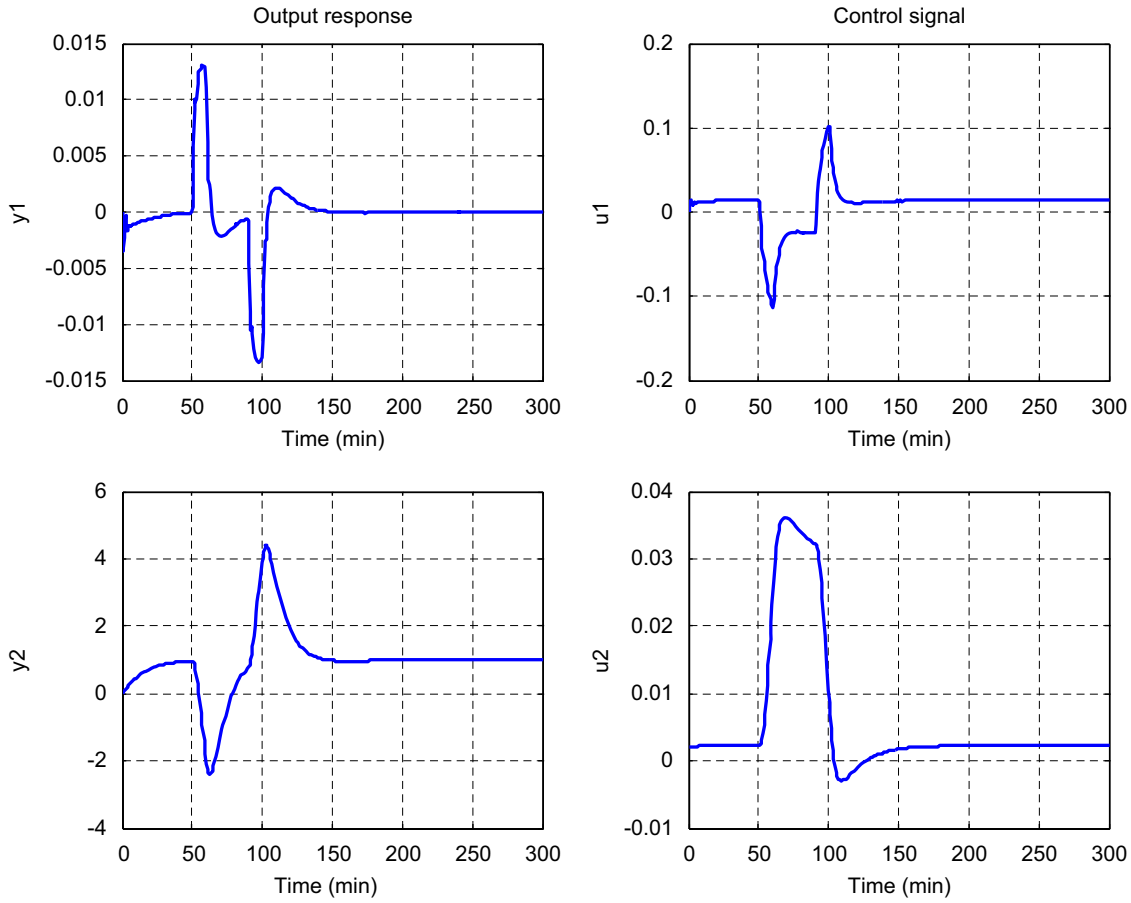


**Fig. 4.** The performance with non-dominant control signal selection for each loop.

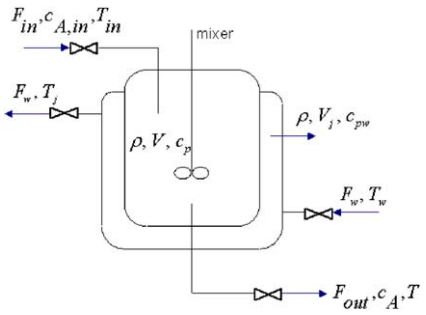


**Fig. 5.** The CSTR diagram [43].

for DDC are: $b_{0,11} = -0.5$, $b_{0,22} = -0.03$. Note that $b_{0,11}$ and $b_{0,22}$ are the approximate values of $b_{11}$ and $b_{22}$ in (15). The two sets of tuning parameters for DDC are: $\omega_{c1} = \omega_{c2} = 0.2$, $\omega_{o1} = \omega_{o2} = 0.03$ and $\omega_{c1} = \omega_{c2} = 1$, $\omega_{o1} = \omega_{o2} = 0.15$, respectively. In addition, a reasonable amount of noise is added to the measurement in simulation. Compared to the signals, the noises are amount to about 1% and 0.1% in the two loops, respectively. The simulation results demonstrate that the nonlinear system is well controlled in the presence of cross-couplings and noises. The performance shows the effects of different controller and observer bandwidths. The larger observer bandwidths result in more accurate estimation, but it also leads to more sensitivity to

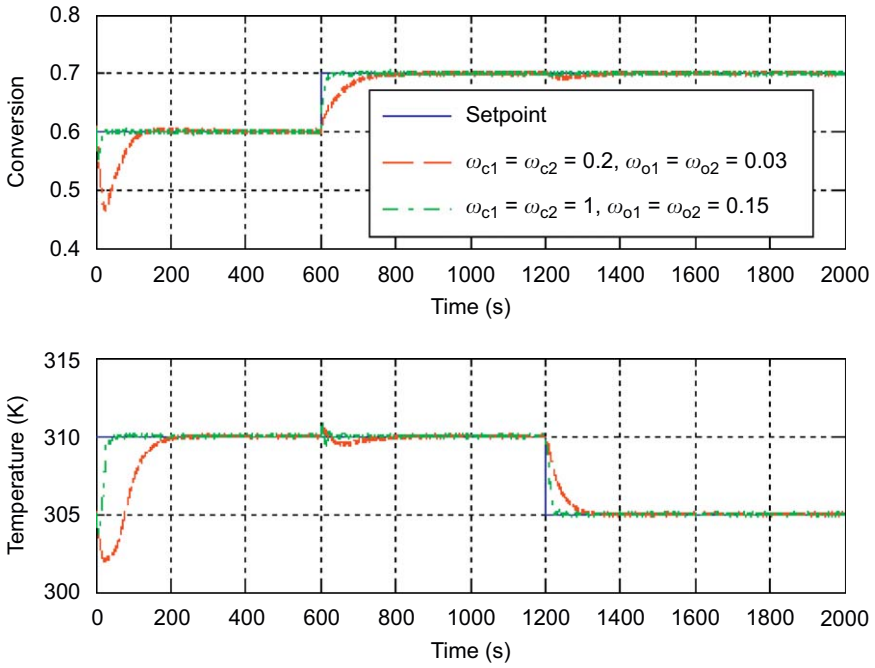


**Fig. 6.** The output response of CSTR under the control of the DDC.

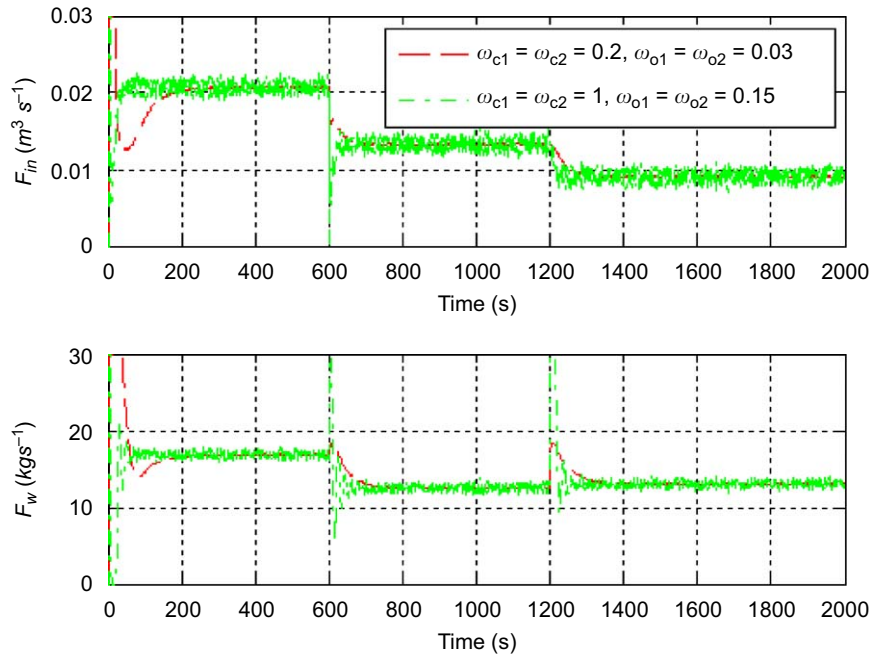


**Fig. 7.** The control signals of CSTR.

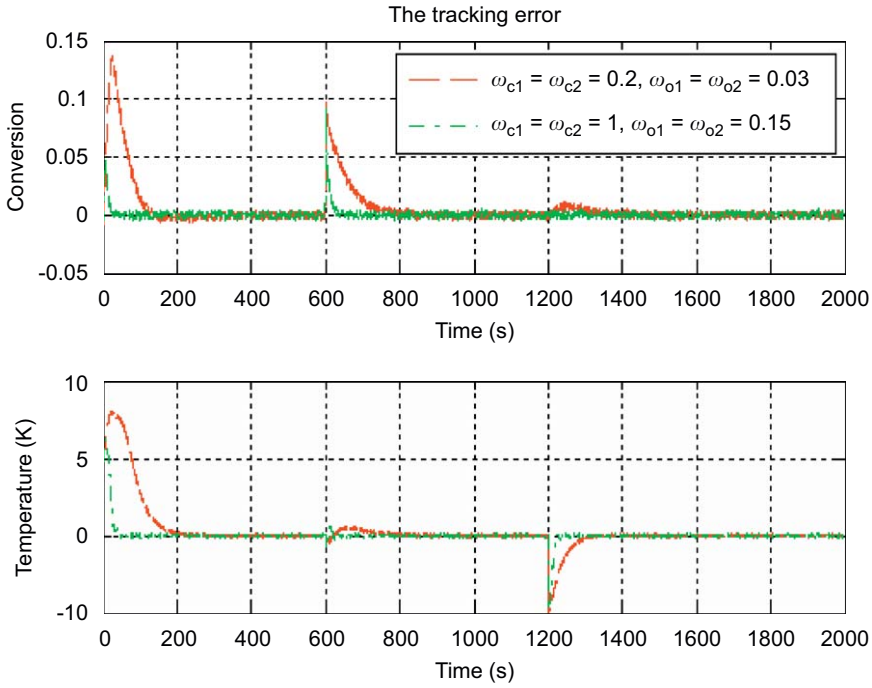


**Fig. 8.** The tracking error of CSTR.

noises. The larger controller bandwidths make the response faster, with a more jittery control signal.

## 4. Concluding remarks

In this paper, a novel disturbance decoupling control method is proposed for a class of square multivariable systems of various orders. It is based on a novel disturbance rejection concept and it does not require an accurate mathematical model. The proposed DDC method is easy to understand and to implement, making it an appealing solution for practitioners. Stability analysis shows that the boundedness of the estimation and closed-loop tracking errors is assured. Furthermore, it is established that the error upper bounds monotonously decrease with the bandwidths. Simulation results are quite promising. Good performance is attained in two case studies involving both the linear and nonlinear multivariable plants with significant uncertainties.

## Appendix A. Stability

In this appendix, how the estimation error of the observer and the closed-loop tracking error behave will be shown.

### A.1. Convergence of the ESO

Let $\tilde{x}_{j,i}(t) = x_{j,i}(t) - \hat{x}_{j,i}(t)$, $j = 1, \ldots, n_i + 1$. From (5) and (6), the observer tracking error dynamics can be shown as

$$\begin{aligned}
&\dot{\tilde{x}}_{1,i} = \tilde{x}_{2,i} - \omega_{o,i}\alpha_{1,i}\tilde{x}_{1,i},\\
&\vdots\\
&\dot{\tilde{x}}_{n_i-1,i} = \tilde{x}_{n_i,i} - \omega_{o,i}^{n_i-1}\alpha_{n_i-1,i}\tilde{x}_{1,i},\\
&\dot{\tilde{x}}_{n_i,i} = \tilde{x}_{n_i+1,i} - \omega_{o,i}^{n_i}\alpha_{n_i,i}\tilde{x}_{1,i},\\
&\dot{\tilde{x}}_{n_i+1,i} = h_i(x_i, w) - \omega_{o,i}^{n_i+1}\alpha_{n_i+1,i}\tilde{x}_{1,i}.
\end{aligned} \tag{16}$$

Now scale the observer tracking error $\tilde{x}_{j,i}(t)$ by $\omega_{o,i}^{j-1}$, i.e. let $\varepsilon_{j,i}(t) = \tilde{x}_{j,i}(t)/\omega_{o,i}^{j-1}$, $j = 1, \ldots, n_i + 1$. Then the error Eq. (16) can be written as

$$\dot{\varepsilon}_i = \omega_{o,i} A\varepsilon_i + B\frac{h_i(x_i, w)}{\omega_{o,i}^{n_i}} \tag{17}$$

where

$$A = \begin{bmatrix} -\alpha_{1,i} & 1 & 0 & \cdots & 0\\ -\alpha_{2,i} & 0 & 1 & \cdots & 0\\ \vdots & \vdots & \ddots & \vdots & \vdots\\ -\alpha_{n_i,i} & 0 & \cdots & 0 & 1\\ -\alpha_{n_i+1,i} & 0 & \cdots & 0 & 0 \end{bmatrix}, \quad B = \begin{bmatrix} 0\\ 0\\ \vdots\\ 0\\ 1 \end{bmatrix}.$$

**Theorem 1.** *Assuming $h_i(x_i, w)$ is bounded, there exist a constant $\sigma > 0$ and a finite $T_1 > 0$ such that $|\tilde{x}_{j,i}(t)| \leqslant \sigma$, $j = 1, 2, \ldots, n_i + 1$, $\forall t \geqslant T_1 > 0$ and $\omega_{o,i} > 0$. Furthermore, $\sigma = O(1/\omega_{o,i}^{\kappa})$, for some positive integer $\kappa$.*

**Proof.** Solving (17), one has

$$\varepsilon_i(t) = e^{\omega_{o,i}At}\varepsilon_i(0) + \int_0^t e^{\omega_{o,i}A(t-\tau)}B\frac{h_i(x_i(\tau), w)}{\omega_{o,i}^{n_i}}\,d\tau. \tag{18}$$

Let

$$p_i(t) = \int_0^t e^{\omega_{o,i}A(t-\tau)}B\frac{h_i(x_i(\tau), w)}{\omega_{o,i}^{n_i}}\,d\tau. \tag{19}$$

Since $h_i(x_i(\tau), w)$ is bounded, that is, $|h_i(x_i(\tau), w)| \leqslant \delta$, where $\delta$ is a positive constant, for $j = 1, 2, \ldots, n_i + 1$, one has

$$\begin{aligned}
|p_{j,i}(t)| &\leqslant \frac{\int_0^t [e^{\omega_{o,i}A(t-\tau)}B]_j |h_i(x_i(\tau), w)|\,d\tau}{\omega_{o,i}^{n_i}}\\
&\leqslant \frac{\delta\int_0^t [e^{\omega_{o,i}A(t-\tau)}B]_j\,d\tau}{\omega_{o,i}^{n_i}}\\
&\leqslant \frac{\delta}{\omega_{o,i}^{n_i+1}}[|(A^{-1}B)_j| + |(A^{-1}e^{\omega_{o,i}At}B)_j|].
\end{aligned} \tag{20}$$

For $A$ and $B$ defined in (17),

$$A^{-1}=\begin{bmatrix} 0 & 0 & 0 & \cdots & -\dfrac{1}{\alpha_{n_i+1,i}} \\ 1 & 0 & 0 & \cdots & -\dfrac{\alpha_{1,i}}{\alpha_{n_i+1,i}} \\ 0 & 1 & 0 & \cdots & -\dfrac{\alpha_{2,i}}{\alpha_{n_i+1,i}} \\ \vdots & \vdots & \vdots & \ddots & \vdots \\ 0 & 0 & \cdots & 1 & -\dfrac{\alpha_{n_i,i}}{\alpha_{n_i+1,i}} \end{bmatrix},$$

and

$$|(A^{-1}B)_j|=\begin{cases} \left.\dfrac{1}{\alpha_{n_i+1,i}}\right|_{j=1} \\ \left.\dfrac{\alpha_{j-1,i}}{\alpha_{n_i+1,i}}\right|_{j=2,\ldots,n_i+1} \end{cases} \leqslant \upsilon \tag{21}$$

where

$$\upsilon=\max_{j=2,\ldots,n_i+1}\left\{\frac{1}{\alpha_{n_i+1,i}},\frac{\alpha_{j-1,i}}{\alpha_{n_i+1,i}}\right\}.$$

According to the selection of $\alpha_{j,i}$, $j=1,2,\ldots,n_i+1$, $A$ is Hurwitz. Therefore there exists a finite time $T_1>0$ such that

$$|[e^{\omega_{o,i}At}]_{jk}|\leqslant\frac{1}{\omega_{o,i}^{n_i+1}} \tag{22}$$

for all $t\geqslant T_1$, $j,k=1,2,\ldots,n_i+1$. Hence

$$|[e^{\omega_{o,i}At}B]_j|\leqslant\frac{1}{\omega_{o,i}^{n_i+1}} \tag{23}$$

for all $t\geqslant T_1$, $j=1,2,\ldots,n_i+1$. Note that $T_1$ depends on $\omega_{o,i}A$. Let

$$A^{-1}=\begin{pmatrix} s_{11} & \cdots & s_{1,n_i+1} \\ \vdots & \ddots & \vdots \\ s_{n_i+1,1} & \cdots & s_{n_i+1,n_i+1} \end{pmatrix} \quad \text{and}$$

$$e^{\omega_{o,i}At}=\begin{bmatrix} d_{11} & \ldots & d_{1,n_i+1} \\ \vdots & \ddots & \vdots \\ d_{n_i+1,1} & \cdots & d_{n_i+1,n_i+1} \end{bmatrix}.$$

One has

$$\begin{aligned} |(A^{-1}e^{\omega_{o,i}At}B)_j| &= |s_{j1}d_{1,n_i+1}+s_{j2}d_{2,n_i+1}+\cdots+s_{j,n_i+1}d_{n_i+1,n_i+1}| \\ &\leqslant\frac{|s_{j1}|+|s_{j2}|+\cdots+|s_{j,n_i+1}|}{\omega_{o,i}^{n_i+1}} \\ &=\begin{cases} \left.\dfrac{1}{\omega_{o,i}^{n_i+1}\alpha_{n_i+1,i}}\right|_{j=1} \\ \left.\dfrac{1}{\omega_{o,i}^{n_i+1}}\left(1+\dfrac{\alpha_{j-1,i}}{\alpha_{n_i+1,i}}\right)\right|_{j=2,\ldots,n_i+1} \end{cases} \\ &\leqslant\frac{\mu}{\omega_{o,i}^{n_i+1}} \end{aligned} \tag{24}$$

for all $t\geqslant T_1$, $j=1,2,\ldots,n_i+1$, where

$$\mu=\max_{j=2,\ldots,n_i+1}\left\{\frac{1}{\alpha_{n_i+1,i}},1+\frac{\alpha_{j-1,i}}{\alpha_{n_i+1,i}}\right\}$$

From (20), (21) and (24), one obtains

$$|p_{j,i}(t)|\leqslant\frac{\delta\upsilon}{\omega_{o,i}^{n_i+1}}+\frac{\delta\mu}{\omega_{o,i}^{2n_i+2}} \tag{25}$$

for all $t\geqslant T_1$, $j=1,2,\ldots,n_i+1$. Let $\varepsilon_{sum,i}(0)=|\varepsilon_{1,i}(0)|+|\varepsilon_{2,i}(0)|+\cdots+|\varepsilon_{n_i+1,i}(0)|$. It follows that

$$\begin{aligned} |[e^{\omega_{o,i}At}\varepsilon_i(0)]_j| &= |d_{j1}\varepsilon_{1,i}(0)+d_{j2}\varepsilon_{2,i}(0)+\cdots+d_{j,n+1}\varepsilon_{n_i+1,i}(0)| \\ &\leqslant\frac{|\varepsilon_{1,i}(0)|+|\varepsilon_{2,i}(0)|+\cdots+|\varepsilon_{n_i+1,i}(0)|}{\omega_{o,i}^{n_i+1}} \\ &=\frac{\varepsilon_{sum,i}(0)}{\omega_{o,i}^{n_i+1}} \end{aligned} \tag{26}$$

for all $t\geqslant T_1$, $j=1,2,\ldots,n_i+1$. From (18), one has

$$|\varepsilon_{j,i}(t)|\leqslant|[e^{\omega_{o,i}At}\varepsilon_i(0)]_j|+|p_{j,i}(t)|. \tag{27}$$

Let $\tilde{x}_{sum,i}(0)=|\tilde{x}_{1,i}(0)|+|\tilde{x}_{2,i}(0)|+\cdots+|\tilde{x}_{n_i+1,i}(0)|$. According to $\varepsilon_{j,i}(t)=\tilde{x}_{j,i}(t)/\omega_{o,i}^{j-1}$ and Eqs. (25)–(27), one has

$$\begin{aligned} |\tilde{x}_{j,i}(t)| &\leqslant\left|\frac{\tilde{x}_{sum,i}(0)}{\omega_{o,i}^{n_i+1}}\right|+\frac{\delta\upsilon}{\omega_{o,i}^{n_i-j+2}}+\frac{\delta\mu}{\omega_{o,i}^{2n_i-j+3}} \\ &=\sigma \end{aligned} \tag{28}$$

for all $t\geqslant T_1$, $j=1,2,\ldots,n_i+1$. □

It has been proven above that in the absence of the plant model, the estimation error of the ESO (5) is bounded and its upper bound monotonously decreases with the observer bandwidth. Regarding the assumption that $h_i(x_i,w)$ is bounded, a motor driven motion control application is given to explain its meaning; it means that the rate of change in acceleration is bounded. Looking at the motor itself, it means that the supply voltage is bounded, which is obviously true. More generally speaking, it means that there is a limit to the rate of change in the physical world, or that no change is instantaneous. When $f_i$ is a composite variable that changes very rapidly, the magnitude of $\dot{f}_i$ can be quite large, though bounded. In this case, the observer bandwidth needs to be sufficiently large for an accurate estimate of $f_i$.

The convergence of DDC, where ESO is employed, is analyzed next.

### A.2. Convergence of the DDC

Assume that the control design objective is to make the output of the plant follow a given, bounded, reference signal $r_i(t)$, whose derivatives, $\dot{r}_i(t),\ddot{r}_i(t),\ldots,r_i^{n_i}(t)$, are also bounded. Let $[r_{1,i},r_{2,i},\ldots,r_{n_i+1,i}]^T=[r_i,\dot{r}_{1,i},\ldots,\dot{r}_{n_i,i}]^T$ and $e_{j,i}(t)=r_{j,i}(t)-x_{j,i}(t)$, $j=1,2,\ldots,n_i$.

**Theorem 2.** *Assuming that $h_i(x_i,w)$ is bounded, there exist a constant $\rho>0$ and a finite time $T_3>0$ such that $|e_{j,i}(t)|\leqslant\rho$, $j=1,2,\ldots,n_i$, $\forall t\geqslant T_3>0$, $\omega_{o,i}>0$ and $\omega_{c,i}>0$. Furthermore, $\rho=O(1/\omega_{c,i}^J)$ for some positive integer $J$.*

**Proof.** From (8) and (10), one has

$$\begin{aligned} u_i &= \frac{k_{1,i}(r_{1,i}-\hat{x}_{1,i})+\cdots+k_{n_i,i}(r_{n_i,i}-\hat{x}_{n_i,i})-\hat{x}_{n_i+1,i}+r_{n_i+1,i}}{b_{ii}} \\ &= \{k_{1,i}[r_{1,i}-(x_{1,i}-\tilde{x}_{1,i})]+\cdots+k_{n_i,i}[r_{n_i,i}-(x_{n_i,i}-\tilde{x}_{n_i,i})] \\ &\quad -(x_{n_i+1,i}-\tilde{x}_{n_i+1,i})+r_{n_i+1,i}\}/b_{ii} \\ &= \frac{k_{1,i}(e_{1,i}+\tilde{x}_{1,i})+\cdots+k_{n_i,i}(e_{n_i,i}+\tilde{x}_{n_i,i})-(x_{n_i+1,i}-\tilde{x}_{n_i+1,i})+r_{n_i+1,i}}{b_{ii}}. \end{aligned} \tag{29}$$

Let $e_i=[e_{1,i},\ldots,e_{n_i,i}]^T\in\mathbb{R}^{n_i}$, $\tilde{x}_i(t)=[\tilde{x}_{1,i},\ldots,\tilde{x}_{n_i+1,i}]^T\in\mathbb{R}^{n_i+1}$. Then

$$\begin{aligned} &\dot{e}_{1,i}=\dot{r}_{1,i}-\dot{x}_{1,i}=r_{2,i}-x_{2,i}=e_{2,i}, \\ &\vdots \\ &\dot{e}_{n_i-1,i}=\dot{r}_{n_i-1,i}-\dot{x}_{n_i-1,i}=r_{n_i,i}-x_{n_i,i}=e_{n_i,i}, \\ &\dot{e}_{n_i,i}=\dot{r}_{n_i,i}-\dot{x}_{n_i,i}=r_{n_i+1,i}-(x_{n_i+1,i}+b_{ii}u_i) \\ &\quad =-k_{1,i}(e_{1,i}+\tilde{x}_{1,i})-\cdots-k_{n_i,i}(e_{n_i,i}+\tilde{x}_{n_i,i})-\tilde{x}_{n_i+1,i}. \end{aligned} \tag{30}$$

From (30), one obtains

$$\dot{e}_i(t) = A_e e_i(t) + A_{\tilde{x}} \tilde{x}_i(t) \tag{31}$$

where

$$A_e = \begin{bmatrix} 0 & 1 & 0 & \cdots & 0 \\ 0 & 0 & 1 & \cdots & 0 \\ \vdots & \vdots & \ddots & \vdots & \vdots \\ 0 & 0 & \cdots & 0 & 1 \\ -k_{1,i} & -k_{2,i} & \cdots & -k_{n_i-1,i} & -k_{n_i,i} \end{bmatrix} \quad \text{and}$$

$$A_{\tilde{x}} = \begin{bmatrix} 0 & 0 & 0 & \cdots & 0 \\ 0 & 0 & 0 & \cdots & 0 \\ \vdots & \vdots & \ddots & \vdots & \vdots \\ 0 & 0 & \cdots & 0 & 0 \\ -k_{1,i} & -k_{2,i} & \cdots & -k_{n_i,i} & -1 \end{bmatrix}.$$

Solving (31), it follows that

$$e_i(t) = e^{A_e t} e_i(0) + \int_0^t e^{A_e(t-\tau)} A_{\tilde{x}} \tilde{x}_i(\tau)\, d\tau. \tag{32}$$

According to (31) and Theorem 1, one has

$$[A_{\tilde{x}} \tilde{x}_i(\tau)]_{j=1,\ldots,n_i-1} = 0$$

$$\begin{aligned} |[A_{\tilde{x}} \tilde{x}_i(\tau)]_{n_i}| &= |-k_{1,i}\tilde{x}_{1,i}(\tau) - \cdots - k_{n_i,i}\tilde{x}_{n_i,i}(\tau) - \tilde{x}_{n_i+1,i}(\tau)| \\ &\leqslant k_{sum,i}\sigma = \gamma \quad \text{for all } t \geqslant T_1 \end{aligned} \tag{33}$$

where $k_{sum,i} = 1 + \sum_{j=1}^{n_i} k_{j,i}$. Let $\varphi_i(t) = \int_0^t e^{A_e(t-\tau)} A_{\tilde{x}} \tilde{x}_i(\tau)\, d\tau$. Define

$$\Psi = \begin{bmatrix} 0 \\ \vdots \\ 0 \\ \gamma \end{bmatrix}.$$

It follows that

$$\begin{aligned} \left|\varphi_{j,i}(t)\right| &= \int_0^t [e^{A_e(t-\tau)} A_{\tilde{x}} \tilde{x}_i(\tau)]_j d\tau \leqslant \int_0^t [e^{A_e(t-\tau)} \Psi]_j\, d\tau \\ &\leqslant |(A_e^{-1}\Psi)_j| + |(A_e^{-1} e^{A_e t}\Psi)_j|. \end{aligned} \tag{34}$$

Since

$$A_e^{-1} = \begin{bmatrix} -\dfrac{k_{2,i}}{k_{1,i}} & -\dfrac{k_{3,i}}{k_{1,i}} & \cdots & -\dfrac{k_{n_i,i}}{k_{1,i}} & -\dfrac{1}{k_{1,i}} \\ 1 & 0 & \cdots & 0 & 0 \\ 0 & 1 & \cdots & 0 & 0 \\ \vdots & \vdots & \ddots & \vdots & \vdots \\ 0 & 0 & \cdots & 1 & 0 \end{bmatrix},$$

one can obtain

$$\begin{aligned} &|(A_e^{-1}\Psi)_1| = \frac{\gamma}{k_{1,i}} = \frac{\gamma}{\omega_{c,i}^{n_i}} \\ &|(A_e^{-1}\Psi)_j||_{j=2,\ldots,n_i} = 0. \end{aligned} \tag{35}$$

Since $A_e$ is Hurwitz, there exists a finite time $T_2 > 0$ such that

$$|[e^{A_e t}]_{jk}| \leqslant \frac{1}{\omega_{c,i}^{n_i+1}} \tag{36}$$

for all $t \geqslant T_2$, $j,k = 1,2,\ldots,n_i$. Note that $T_2$ depends on $A_e$. Let

$$e^{A_e t} = \begin{bmatrix} o_{11} & \cdots & o_{1n} \\ \vdots & \ddots & \vdots \\ o_{n1} & \cdots & o_{nn} \end{bmatrix} \quad \text{and}$$

$$e_{sum,i}(0) = |e_{1,i}(0)| + |e_{2,i}(0)| + \cdots + |e_{n_i,i}(0)|.$$

It follows that

$$\begin{aligned} |[e^{A_e t} e_i(0)]_j| &= |o_{j1}e_{1,i}(0) + o_{j2}e_{2,i}(0) + \cdots + o_{j,n_i}e_{n_i,i}(0)| \\ &\leqslant |o_{j1}e_{1,i}(0)| + |o_{j2}e_{2,j}(0)| + \cdots + |o_{j,n_i}e_{n_i,i}(0)| \\ &\leqslant \frac{|e_{1,i}(0)| + |e_{2,i}(0)| + \cdots + |e_{n_i,i}(0)|}{\omega_{c,i}^{n_i+1}} \\ &= \frac{e_{sum,i}(0)}{\omega_{c,i}^{n_i+1}} \end{aligned} \tag{37}$$

for all $t \geqslant T_2$, $j = 1,2,\ldots,n_i$. Let $T_3 = \max\{T_1, T_2\}$. One has

$$|(e^{A_e t}\Psi)_j| \leqslant \frac{\gamma}{\omega_{c,i}^{n_i+1}} \tag{38}$$

for all $t \geqslant T_3$, $j = 1,2,\ldots,n_i$, and

$$|(A_e^{-1} e^{A_e t}\Psi)_j| \leqslant \begin{cases} \left.\dfrac{1 + \sum_{i=2}^{n_i} k_{j,i}}{\omega_{c,i}^{n_i}} \dfrac{\gamma}{\omega_{c,i}^{n_i+1}}\right|_{j=1} \\ \left.\dfrac{\gamma}{\omega_{c,i}^{n_i+1}}\right|_{j=2,\ldots,n_i} \end{cases} \tag{39}$$

for all $t \geqslant T_3$. From (34), (35), and (39), one obtains

$$|\varphi_{j,i}(t)| \leqslant \begin{cases} \left.\dfrac{\gamma}{\omega_{c,i}^{n_i}} + \dfrac{1 + \sum_{j=2}^{n_i} k_{j,i}}{\omega_{c,i}^{n_i}} \dfrac{\gamma}{\omega_{c,i}^{n_i+1}}\right|_{j=1} \\ \left.\dfrac{\gamma}{\omega_{c,i}^{n_i+1}}\right|_{j=2,\ldots,n_i} \end{cases} \tag{40}$$

for all $t \geqslant T_3$. From (32), one has

$$|e_{j,i}(t)| \leqslant |[e^{A_e t} e_i(0)]_j| + |\varphi_{j,i}(t)|. \tag{41}$$

According to (37), (40)–(41), one has

$$\begin{aligned} |e_{j,i}(t)| &\leqslant \begin{cases} \left.\dfrac{e_{sum,i}(0)}{\omega_{c,i}^{n_i+1}} + \dfrac{\gamma}{\omega_{c,i}^{n_i}} + \dfrac{1 + \sum_{j=2}^{n_i} k_{j,i}}{\omega_{c,i}^{n_i}} \dfrac{\gamma}{\omega_{c,i}^{n_i+1}}\right|_{j=1} \\ \left.\dfrac{e_{sum,i}(0) + \gamma}{\omega_{c,i}^{n_i+1}}\right|_{j=2,\ldots,n_i} \end{cases} \\ &\leqslant \rho \end{aligned} \tag{42}$$

for all $t \geqslant T_5$, $j = 1,2,\ldots,n_i$, where

$$\rho = \max\left\{\frac{e_{sum,i}(0)}{\omega_{c,i}^{n_i+1}} + \frac{\gamma}{\omega_{c,i}^{n_i}} + \frac{1 + \sum_{j=2}^{n_i} k_{j,i}}{\omega_{c,i}^{n_i}} \frac{\gamma}{\omega_{c,i}^{n_i+1}}, \frac{e_{sum,i}(0) + \gamma}{\omega_{c,i}^{n_i+1}}\right\}. \qquad \square$$

It has been shown above that, with plant dynamics largely unknown, the tracking error of the DDC and its up to $(n-1)$th order derivatives are bounded and their upper bounds monotonously decrease with the observer and controller bandwidths.

In summary, the proposed DDC approach, as shown above, renders a new alternative for decoupling control problems. With the convergence of ESO and the stability analysis of ADRC shown above, the chief contribution of this paper is to present that the decoupling problems can be reformulated as a disturbance rejection one, without an elaborate plant model. In fact, the only information required is the orders of the subsystems associated with each input–output pair and the values of the corresponding

input gains $b_{ii}$. Even when $b_{ii}$ are unknown, the DDC method can still be implemented with the approximate $b_{ii}$ as the tuning parameters [24–26]. Being able to deal with multivariable systems that have different orders for different input–output parings is another advantage of the proposed method. Overall, the DDC is a conceptually simple and easy to understand, and above all, practical solution for real world decoupling problems, where there is a large amount of uncertainties.

## Appendix B. The description of variables for the CSTR Model (Roffel & Betlem, 2004)

| Variable | Value | Unit | Description |
|---|---|---|---|
| $F_{in}$ | | $kg\,s^{-1}$ | The reactant feed flow rate |
| $F_{out}$ | | $kg\,s^{-1}$ | The outlet flow rate |
| $V$ | 1 | $m^3$ | The volume of the tank reactor |
| $c_A$ | | $kg\,m^{-3}$ | The concentration of species A inside the tank |
| $c_{A,in}$ | 866 | $kg\,m^{-3}$ | The concentration of species A at the feed |
| $c_{A,out}$ | | $kg\,m^{-3}$ | The concentration of species A at the outlet |
| $k_0$ | $4\times10^8$ | $s^{-1}$ | Arrhenius rate constant |
| $E$ | $6\times10^4$ | $J\,mol^{-1}\,K^{-1}$ | Activation energy |
| $R$ | 8.314 | $J\,mol^{-1}\,K^{-1}$ | Gas law constant |
| $T$ | | K | Reactor temperature |
| $\rho$ | 866 | $kg\,m^{-3}$ | Density of the reactant |
| $C_p$ | 1.791 | $J\,kg^{-1}\,K^{-1}$ | Specific heat capacity of species $A$ and $B$ |
| $T_{in}$ | 293 | K | Temperature of the inlet stream |
| $U$ | 30 | $W\,m^{-2}\,K^{-1}$ | Overall heat transfer coefficient |
| $A$ | 50 | $m^2$ | Heat transfer area |
| $\Delta H$ | −140 | $J\,kg^{-1}$ | Heat of reaction |
| $T_j$ | | K | Temperature of the cooling jacket |
| $V_j$ | 0.2 | $m^3$ | Volume of the cooling jacket |
| $\rho_w$ | 998 | $kg\,m^{-3}$ | Density of the water |
| $C_{pw}$ | 4.181 | $J\,kg^{-1}\,K^{-1}$ | Specific heat capacity of water |
| $F_w$ | | $kg\,s^{-1}$ | Coolant water mass rate at the inlet and the outlet |
| $T_w$ | 290 | K | Coolant water temperature at the jacket inlet |

## References


Astrom, K. J., & Hagglund, T. (1995). *PID controllers: Theory, design, and tuning*. Research Triangle Park, NC: Instrument Society of America.

Dayal, B. S., & MacGregor, J. F. (1997). Recursive exponentially weighted PLS and its application to adaptive control and prediction. *Journal of Process Control*, *7*(3), 169–179.

Descusse, J. (1991). Block noninteracting control with regular static state feedback: A complete solution. *Automatica*, *27*, 883–886.

Gao, Z. (2003). Scaling and parameterization based controller tuning. In *Proceedings of the 2003 American control conference* (pp. 4989–4996). Denver, CO, USA.

Gao, Z. (2006). Active disturbance rejection control: A paradigm shift in feedback control system design. In *Proceedings of the 2006 American control conference* (pp. 2399–2405). Minneapolis, MN, USA.

Gao, Z., Huang, Y., & Han, J. (2001). An alternative paradigm for control system design. In *Proceedings of the 40th IEEE conference on decision and control* (pp. 4578–4585). Orlando, FL, USA.

Gilbert, E. G. (1969). The decoupling of multivariable systems by state feedback. *SIAM Journal on Control*, *7*(1), 50–63.

Han, J. (1998). Auto-disturbance rejection control and its applications. *Control and Decision*, *13*(1), 19–23 (In Chinese).

Han, J. (1999). Nonlinear design methods for control systems. In *Proceedings of the 14th IFAC world congress*. Beijing, PRC.

Huang, Y., Xu, K., Han, J., & Lam, J. (2001). Flight control design using extended state observer and non-smooth feedback. In *Proceedings of the 40th IEEE conference on decision and control* (pp. 223–228). Orlando, FL, USA.

Johnson, C. (1976). Theory of disturbance-accommodating controllers. *Control and Dynamic Systems*, *12*, 387–489.

Kwon, S., & Chung, W. K. (2003). A discrete-time design and analysis of perturbation observer for motion control applications. *IEEE Transactions on Control Systems Technology*, *11*(3), 399–407.

Lu, Y. S. (2008). Smooth speed control of motor drives with asymptotic disturbance compensation. *Control Engineering Practice*, *16*(5), 597–608.

Luyben, W. L. (1990). *Process modeling, simulation, and control for chemical engineers*. New York: McGraw-Hill.

Miklosovic, R., & Gao, Z. (2005). A dynamic decoupling method for controlling high performance turbofan engines. In *Proceedings of the 16th IFAC world congress*. Prague, Czech Republic.

Morgan, B. S. (1964). The synthesis of linear multivariable systems by state variable feedback. *IEEE Transactions on Automatic Control*, *AC-9*, 404–411.

Morse, A. S., & Wonham, W. A. (1970). Decoupling and pole assignment by dynamic compensation. *SIAM Journal on Control*, *8*, 317–337.

Roffel, B., & Betlem, B. H. (2004). *Advanced practical process control*. Berlin: Springer.

Schrijver, E., & van Dijk, J. (2002). Disturbance observers for rigid mechanical systems: Equivalence, stability, and design. *ASME Journal of Dynamics Systems, Measurement, and Control*, *124*(4), 539–548.

Su, Y. X., Duan, B. Y., Zheng, C. H., Zhang, Y. F., Chen, G. D., & Mi, J. W. (2004). Disturbance-rejection high-precision motion control of a Stewart platform. *IEEE Transactions on Control System Technology*, *12*(3).

Takatsu, H., & Itoh, T. (1999). Future needs for control theory in industry—report of the control technology survey in Japanese industry. *IEEE Transactions on Control System Technology*, *7*(3), 298–305.

Wang, Q. (2003). *Decoupling control*. Berlin: Springer.

Williams, T. W. C., & Antsaklis, P. J. (1986). A unifying approach to the decoupling of linear multivariable systems. *International Journal of Control*, *44*, 181–201.

Wood, R. K., & Berry, M. W. (1973). Terminal composition control of a binary distillation column. *Chemical Engineering Science*, *28*, 1707–1717.

Yang, Y. P., & Lo, C. P. (2008). Current distribution control of dual directly driven wheel motors for electric vehicles. *Control Engineering Practice*, *16*(11), 1285–1292.

Zheng, Q., & Gao, Z. (2006). Motion control optimization: Problem and solutions. *International Journal of Intelligent Control and Systems*, *10*(4), 269–276.

Zheng, F., Wang, Q. G., & Lee, T. H. (2002). On the design of multivariable PID controllers via LMI approach. *Automatica*, *38*, 517–526.